EEG-based BCI System for Classifying Motor Imagery Tasks of the Same Hand Using Empirical Mode Decomposition

Rami Alazrai[1], Sarah Aburub[1], Farah Fallouh[1], and Mohammad I. Daoud[1]

[1] School of Electrical Engineering and Information Technology, German Jordanian University, Amman, 11180 Jordan
rami.azrai@gju.edu.jo, s.aburub@gju.edu.jo, f.fallouh@gju.edu.jo, mohammad.aldaoud@gju.edu.jo

Abstract

In this paper, we present an EEG-based brain-computer interface (BCI) system for classifying motor imagery (MI) tasks of the same hand using empirical mode decomposition (EMD) method. The EMD method is employed to decompose the EEG signals into a set of intrinsic mode functions (IMFs). Then, a set of features is extracted from the obtained IMFs. These features are used to construct a three-layer hierarchical classification model to discriminate between four MI tasks of the same hand, namely rest, wrist-related tasks, finger-related task, and grasp-related task. In order to evaluate the performance of the proposed approach, we have collected EEG signals for 18 able-bodied subjects while imaging to perform the four MI tasks. Experimental results demonstrate the efficacy of the proposed approach in decoding MI tasks of the same hand based on analyzing EEG signals using the EMD method.

1. Introduction

A brain-computer interface (BCI) is an emerging technology that aims at providing people who are suffering from severe motor impairments with the ability to communicate with their surroundings via analyzing brain signals. Several invasive and noninvasive neuroimaging techniques have been utilized in BCI systems to record brain activities, such as functional magnetic resonance imaging (fMRI), electrocorticographic (ECoG), electroencephalography (EEG), and magnetoencephalography (MEG). Among these different neuroimaging techniques, EEG is considered the most commonly used technique in BCI systems [1]. This is due to many factors, including the high temporal resolution of the EEG signals, high portability, noninvasive nature, and low cost of the recording equipment [1, 2].

During the last two decades, researchers have utilized motor imagery (MI), which is the process of imagining a motor act without actually performing it, to design EEG-based BCI systems that allow individuals with motor disabilities to control various assistive devices, such as wheelchairs [3], prosthetic devices [4], and computers [5]. Nonetheless, the majority of the existing MI EEG-based BCI systems have a limited control dimensions. In particular, these EEG-based BCI systems were designed to discriminate between four classes of MI tasks that are associated with four different body-parts [6–9], including feet, left hand, right hand, and tongue.

Despite the significant efforts invested in classifying MI tasks associated with different body-parts, few researchers have pursued classifying MI tasks within the same hand in order to increase the control dimensions of EEG-based BCI systems. Discriminating between MI tasks of the same hand based on analyzing EEG signals is considered challenging [10–13]. This can be attributed to the low spatial resolution and the non-stationary nature of the EEG signals. In particular, the low spatial resolution of the EEG signals reduces the capability to discriminate between MI tasks of the same hand that activate close regions in the brain [11]. Moreover, the non-stationary nature of the EEG signals implies that the spectral characteristics of the EEG signals are changing as a function of time. Therefore, traditional time-domain and frequency-domain analyses, which are employing the time-invariance assumption, are considered inadequate to analyze EEG signals [14, 15].

In this study, we explore the possibility of utilizing the empirical mode decomposition (EMD) [16] method as a time-frequency analysis of the EEG signals in order to classify MI tasks of the same hand. In particular, EEG data was recorded for 18 able-bodied subjects while imagining to perform four MI tasks using their right hands. The hand MI tasks considered in this study are the rest state, wrist-related tasks, fingers-related tasks, and grasp-related tasks. Then, the EMD method is used to decompose the acquired EEG signals of each subject into several intrinsic mode functions (IMFs). The computed IMFs are segmented into non-overlapping EEG segments, and a set of features, including the variance, skewness, kurtosis, spectral flux, spectral flatness, and Renyi entropy, are extracted from each EEG segment to represent the different classes of MI tasks. The extracted features are utilized to build a three-layer hierarchical classification model that classifies each EEG segment into one of the four MI tasks. Each classification layer is realized using a binary support vector machine (SVM) classifier with a Gaussian radial basis function (RBF) kernel. Experimental results show that the performance of the proposed three-layer classification model outperforms the performance obtained using traditional multi-class SVM classifier. To the best of our knowledge, this is the first study that explores the use of EMD for classifying MI tasks within the same hand.

The remainder of the paper is organized as follows: Section 2 describes the recorded EEG dataset, analysis of the EEG signals using the EMD method, feature extraction, and classification of the MI tasks. Section 3 presents the experimental results. In Section 4, we conclude our final thoughts and address future endeavors.

2. Materials and Methods

2.1. Experimental Procedure

In this study, EEG signals were acquired from 18 able-bodied subjects (6 female subjects) while imagining to perform four types of hand MI tasks using their right hands. In particular, the hand MI tasks considered in this study are the rest state, wrist-related tasks, finger-related tasks, and grasp-related tasks. All subjects gave written informed consent before participating in the experimental procedure. Furthermore, the experimental procedure in this study was approved by the Research Ethics Committee at the German Jordanian University.

During the experiment, each subject was asked to sit comfortably on a chair and to rest his/her arms on a desk located in front of him/her. After that, a computer monitor is used to display visual cues that instruct the subject to imagine performing one of the four hand MI tasks. The duration of the visual cue was equal to 3 seconds, while the duration of the imagination was equal to 7 seconds. Each subject was asked to repeat each MI task 7 times.

2.2. Data Acquisition and Preprocessing

Raw EEG data was acquired using the BioSemi ActiveTwo EEG system (Biosemi B.V., Amsterdam, Netherlands). The EEG signals were recorded at a sampling rate of 2048 samples/second using 16 Ag/AgCl electrodes arranged according to the $10-20$ international system, as shown in Fig. 1. In this study, we have selected a subset of five EEG channels, namely C_3, C_z, C_4, P_z and F_z, that are highly correlated with MI brain activities [6].

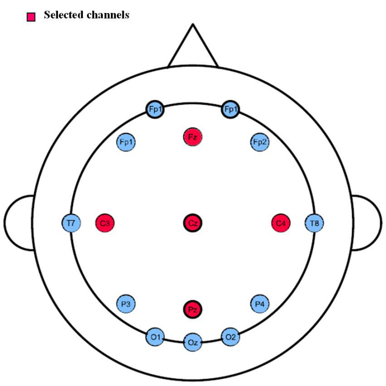

Figure 1. The positions of the EEG electrodes employed in this study arranged according to the 10-20 EEG system.

The acquired EEG signals are preprocessed by reducing the sampling rate to 256 samples/second. Furthermore, a band pass filter with a bandwidth of 0.5 - 35 Hz is applied to the EEG signals. In addition, the effect of muscle and electrooculography (EOG) artifacts was reduced using both the EEGLab and the automatic artifact removal (AAR) toolboxes [17, 18].

2.3. Time-Frequency Analysis and Feature Extraction

Empirical mode decomposition (EMD) is a method that decomposes a time domain signal into a set of intrinsic mode functions (IMFs). Unlike the legacy Fourier and Wavelet transforms, EMD provides a detailed time frequency analysis of the signal without the need for a priori defined basis function [19]. Furthermore, utilizing the EMD method to perform time-frequency analysis enables to capture the nonlinear and non-stationary characteristics of the EEG signals [20]. The EMD method employs a sifting process to decompose the oscillatory time-domain signal into AM-FM components [21]. The steps involved in applying the sifting process to an EEG time series input signal $g(t)$ are described as follows [22, 23]:

I. Compute the maxima and minima points of $g(t)$. Then, interpolate between the maxima points to find an upper envelope of $g(t)$. Similarly, interpolate between the minima points to find a lower envelope of $g(t)$.

II. Calculate the mean of the upper and lower envelopes $m(t)$.

III. Compute the signal $c(t)$ by subtracting $m(t)$ from $g(t)$. Then, check if $c(t)$ satisfies the conditions of an IMF. Specifically, in order to consider $c(t)$ as an IMF, $c(t)$ has to satisfy the following conditions:

- The number of extreme and zero-crossings must be equal or differ at most by one.
- At any point, the mean value of the envelope defined by the local maxima and the envelope defined by the local minima is equal to zero.

IV. If $c(t)$ is an IMF, compute the residue signal $r(t) = g(t) - c(t)$ and set $g(t)$ to be equal to $r(t)$. Then, repeat the first three steps of the sifting process. Otherwise, if $c(t)$ is not an IMF, set $g(t)$ to be equal to $c(t)$ and repeat the first three steps of the sifting process.

V. Repeat the sifting process until no more IMFs can be generated from the residue signal $r(t)$.

Thus, a signal $g(t)$ can be represented as follows:

$$g(t) = \sum_{i=1}^{I} IMF_i + r(t) \tag{1}$$

Where I is the number of IMFs computed for the signal $g(t)$. In this study, we applied the EMD method to the preprocessed EEG signals to obtain a set of IMFs for each of the five channels described in subsection 2.2. Moreover, for each EEG channel, the first three IMFs, namely IMF_1, IMF_2, and IMF_3, were chosen for further processing and feature extraction [24].

After processing the EEG signals using the EMD method, feature vectors are extracted from IMF_1, IMF_2, and IMF_3. Specifically, each IMF is divided into non-overlapping windows of size 128 samples. Then, a set of features that are commonly used for EEG signal analysis are extracted from each window [25]. Table 1 provides a list of the extracted features along with their mathematical representations.

2.4. Classification

In this paper, we propose a three-layer hierarchical classification model to classify each feature vector into one of the four hand MI tasks considered in our study. Specifically, the first layer classifies feature vectors into rest and non-rest MI tasks. Then, the feature vectors that were classified as non-rest at the first layer are passed on to the second layer to identify whether the MI task associated with each vector is a grasp-related task or non-grasp task. Finally, at the third layer, feature vectors that were classified as non-grasp MI task at the second layer are classified into finger-related and wrist-related MI tasks. Figure 2 provides a schematic diagram of the proposed three-layer hierarchical classification model.

Table 1. The extracted features from each IMF at each window position.

Feature	Mathematical formula	Description
Variance	$\sigma^2 = \frac{1}{N}\sum_{j=1}^{N}(W(j)-\mu)^2$	The variance of an EEG segment covered by the window W, where $W(j)$ is the j^{th} time sample of W, μ is the mean of the values within W, and N is the number of samples in W.
Skewness	$\gamma = \frac{1}{N(\sigma^2)^{\frac{3}{2}}}\sum_{j=1}^{N}(W(j)-\mu)^3$	The skewness of an EEG segment covered by the window W.
Kurtosis	$K = \frac{1}{N(\sigma^2)^2}\sum_{j=1}^{N}(W(j)-\mu)^4$	The kurtosis of an EEG segment covered by the window W.
Spectral flux [19]	$SL = \sum_{k=1}^{M}\left(\lvert Z_W^{(l)}(k)\rvert - \lvert Z_W^{(l-1)}(k)\rvert\right)^2$	The spectral flux of an EEG segment covered by the window W. $\lvert Z_W^{(l)}(\cdot)\rvert$ and $\lvert Z_W^{(l-1)}(\cdot)\rvert$ are the magnitudes of the Fourier transform at window positions l and $l-1$, respectively. M is the number of frequency-domain samples.
Spectral flatness [19]	$SF = M\left(\prod_{k=1}^{M}\lvert Z_W(k)\rvert\right)^{\frac{1}{M}}\left(\prod_{k=1}^{M}\lvert Z_W(k)\rvert\right)^{-1}$	The spectral flatness of an EEG segment covered by the window W, where $\lvert Z_W(\cdot)\rvert$ represents the magnitude of the Fourier transform of W.
Renyi entropy [15]	$RE = \frac{1}{1-\alpha}\ln\left(\sum_{k=1}^{M}\left(\frac{\lvert Z_W(k)\rvert}{\sum_{k=1}^{M}\lvert Z_W(k)\rvert}\right)^{\alpha}\right)$	The Renyi entropy of an EEG segment covered by the window W. The parameter α is selected to be equal to 3.

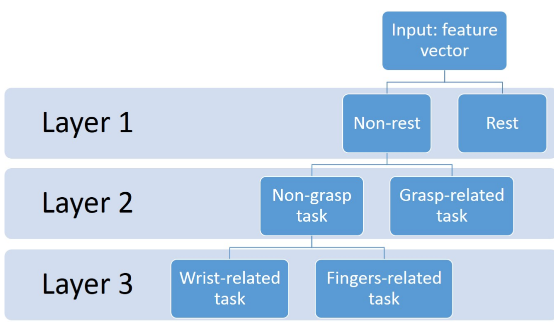

Figure 2. Schematic diagram of the proposed three-layer hierarchical classification model.

In this study, each classification layer was implemented using binary SVM classifiers with RBF kernel [26]. The performance of the SVM classifier with RBF kernel depends on the selected values of the RBF kernel parameter (σ) and the regularization parameter ($C > 0$) [6, 27]. To tune these two parameters, we perform a grid-based search [28, 29] along two directions to determine the values of σ and C for each classification node. In the first direction, we vary the value of the parameter σ, while in the second direction we vary the value of the parameter C. Then, the best SVM model is selected such that its parameters maximize the average classification accuracy.

3. Experimental Results and Discussion

In order to quantify the performance of the proposed approach, we utilize the average classification accuracy as a standard evaluation metric to measure the performance of each layer of the proposed hierarchial classification model. The accuracy can be defined as follows [27]:

$$Accuracy = \frac{(TP+TN)}{(TP+TN+FP+FN)}, \quad (2)$$

where TP represents the number of true positive cases, TN represents the number of true negative cases, FP is the number of false positive cases, and FN represents the number of false negative cases. Furthermore, we compare the obtained performance of our proposed hierarchical classification model with the performance obtained using traditional multi-class SVM classifier with RBF kernel function. In both classification models, namely the hierarchical classification model and the single multi-class model, we compute the accuracy based on utilizing a 10-fold cross-validation procedure [6]. In particular, we randomly divide the feature vectors associated with the four hand MI tasks performed by each subject into 10 folds. Nine folds are used to train the classifiers in each approach, while the remaining fold is used for testing. This procedure is repeated for ten times, and the overall accuracy is computed by averaging the results obtained from each repetition. The results of each classification model are described in the following subsections.

3.1. Results of the Hierarchical Classification Model

Figure 3 shows the average classification accuracy of the first layer computed based on utilizing the feature vectors extracted from each IMF for each subject. The average accuracy$\pm$ standard deviation of the first layer computed over the eighteen subjects for IMF_1, IMF_2, and IMF_3 were 0.78 ± 0.08, 0.72 ± 0.04, and 0.67 ± 0.03, respectively. The results presented in Fig. 3 indicate that the best performance of the first layer was achieved using the feature vectors extracted from IMF_1.

Figure 4 presents the average classification accuracy of the second layer in discriminating between grasp and non-grasp MI tasks for each subject using each of the three IMFs. The average accuracy$\pm$ standard deviation of the second layer computed over the eighteen subjects for IMF_1, IMF_2, and IMF_3 were 0.68 ± 0.08, 0.67 ± 0.07, and 0.66 ± 0.05, respectively. Similar to the results obtained for the first layer, Fig. 4 indicates that the best performance of the second layer was achieved using the feature vectors extracted from IMF_1.

Figure 5 shows the obtained average classification accuracy of the third layer in discriminating between wrist- and fingers-related MI tasks for each subject using each of the three IMFs. The average accuracy$\pm$ standard deviation of the third layer computed over the eighteen subjects for IMF_1, IMF_2, and IMF_3 were 0.67 ± 0.11, 0.68 ± 0.08, and 0.58 ± 0.13, respectively. The results obtained for the third layer indicate that using the features extracted from IMF_2 achieved a slightly better performance compared with the results obtained using the features extracted from IMF_1. On the other hand, using the features extracted from IMF_3, the performance of the third layer has reduced to 0.58 ± 0.13.

The overall average accuracy of the three layers for IMF_1, IMF_2, and IMF_3 were 0.71, 0.69, and 0.64, respectively. These results indicate that the performance of our proposed hierarchical classification model is above the average random classification accuracy, which is equal to 25%.

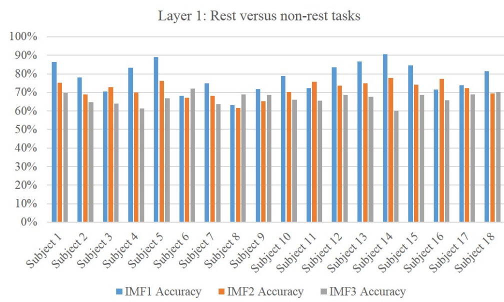

Figure 3. Results of the first layer in our proposed hierarchical classification model.

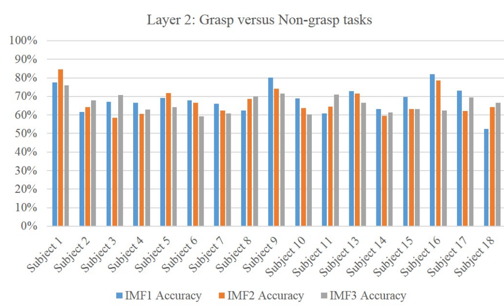

Figure 4. Results of the second layer in our proposed hierarchical classification model.

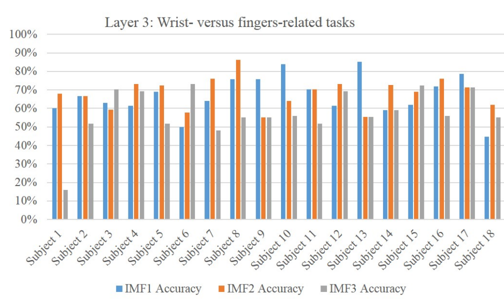

Figure 5. Results of the third layer in our proposed hierarchical classification model.

3.2. Results of the Traditional Multi-Class Classification Model

In order to compare the performance of our proposed three-layer hierarchical classification model with the traditional multi-class classification model, we have constructed a multi-class SVM classifier to classify feature vectors into one of the four MI tasks using the one-versus-one scheme. Figure 6 shows the average classification accuracy obtained using each of the three IMFs for each subject. The average accuracy$\pm$ standard deviation of the multi-class SVM model computed over the eighteen subjects for IMF_1, IMF_2, and IMF_3 were 00.5 ± 0.065, 0.48 ± 0.067, and 0.44 ± 0.07, respectively. In comparison with the results presented in subsection 3.1, our proposed hierarchical classification model has significantly outperformed the performance of the traditional multi-class classification model.

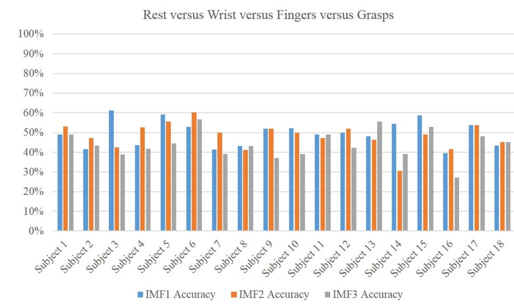

Figure 6. Results of the multi-class SVM classifier for each of the three IMFs.

4. Conclusion and Future Work

In this paper, we investigated the possibility of classifying four MI tasks of the same hand based on analyzing EEG signals using the EMD method. The proposed approach employed the EMD method to decompose the EEG signals into three IMFs. Then, a set of features was extracted from the IMFs and used to build a three-layer hierarchical classification model to discriminate between rest, wrist-related MI tasks, finger-related MI tasks, and grasp-related MI tasks. Experimental results show that our proposed three-layer hierarchical classification model yielded promising results with an overall average accuracy of 71% based on the features extracted from IMF_1. In future work, we intend to expand our proposed hierarchical classification model to include subcategories of the considered hand MI tasks in this study. Moreover, we plan to perform feature analysis in order to investigate the possibility and efficacy of representing the EEG signals using other features extracted from the computed IMFs.

5. Acknowledgment

This work is supported by the Scientific Research Support Fund - Jordan (Grant no. ENG/1/9/2015).

6. References

[1] L. Qin, L. Ding, and B. He, “Motor imagery classification by means of source analysis for brain–computer interface applications,” *Journal of neural engineering*, vol. 1, no. 3, p. 135, 2004.

[2] L. F. Nicolas-Alonso and J. Gomez-Gil, “Brain computer interfaces, a review,” *Sensors*, vol. 12, no. 2, pp. 1211–1279, 2012.

[3] E. W. Sellers, T. M. Vaughan, and J. R. Wolpaw, “A brain-computer interface for long-term independent home use,” *Amyotrophic lateral sclerosis*, vol. 11, no. 5, pp. 449–455, 2010.

[4] G. Pfurtscheller, C. Guger, G. Müller, G. Krausz, and C. Neuper, "Brain oscillations control hand orthosis in a tetraplegic," *Neuroscience letters*, vol. 292, no. 3, pp. 211–214, 2000.

[5] R. Scherer, G. Muller, C. Neuper, B. Graimann, and G. Pfurtscheller, "An asynchronously controlled eeg-based virtual keyboard: improvement of the spelling rate," *IEEE Transactions on Biomedical Engineering*, vol. 51, no. 6, pp. 979–984, 2004.

[6] R. Alazrai, H. Alwanni, Y. Baslan, N. Alnuman, and M. I. Daoud, "Eeg-based brain-computer interface for decoding motor imagery tasks within the same hand using choi-williams time-frequency distribution," *Sensors*, vol. 17, no. 9, p. 1937, 2017.

[7] A. Vuckovic and F. Sepulveda, "Delta band contribution in cue based single trial classification of real and imaginary wrist movements," *Medical & biological engineering & computing*, vol. 46, no. 6, pp. 529–539, 2008.

[8] A. S. Royer, A. J. Doud, M. L. Rose, and B. He, "Eeg control of a virtual helicopter in 3-dimensional space using intelligent control strategies," *IEEE Transactions on neural systems and rehabilitation engineering*, vol. 18, no. 6, pp. 581–589, 2010.

[9] K. LaFleur, K. Cassady, A. Doud, K. Shades, E. Rogin, and B. He, "Quadcopter control in three-dimensional space using a noninvasive motor imagery-based brain–computer interface," *Journal of neural engineering*, vol. 10, no. 4, p. 046003, 2013.

[10] S. Ge, R. Wang, and D. Yu, "Classification of four-class motor imagery employing single-channel electroencephalography," *PloS one*, vol. 9, no. 6, p. e98019, 2014.

[11] K. Liao, R. Xiao, J. Gonzalez, and L. Ding, "Decoding individual finger movements from one hand using human eeg signals," *PloS one*, vol. 9, no. 1, p. e85192, 2014.

[12] X. Yong and C. Menon, "Eeg classification of different imaginary movements within the same limb," *PLoS One*, vol. 10, no. 4, Apr. 2015.

[13] B. J. Edelman, B. Baxter, and B. He, "Eeg source imaging enhances the decoding of complex right-hand motor imagery tasks," *IEEE Transactions on Biomedical Engineering*, vol. 63, no. 1, pp. 4–14, 2016.

[14] B. Boashash, G. Azemi, and J. M. O'Toole, "Time-frequency processing of nonstationary signals: Advanced tfd design to aid diagnosis with highlights from medical applications," *IEEE Signal Processing Magazine*, vol. 30, no. 6, pp. 108–119, 2013.

[15] B. Boashash and S. Ouelha, "Automatic signal abnormality detection using time-frequency features and machine learning: A newborn eeg seizure case study," *Knowledge-Based Systems*, vol. 106, pp. 38–50, 2016.

[16] N. E. Huang, Z. Shen, S. R. Long, M. C. Wu, H. H. Shih, Q. Zheng, N.-C. Yen, C. C. Tung, and H. H. Liu, "The empirical mode decomposition and the hilbert spectrum for nonlinear and non-stationary time series analysis," in *Proceedings of the Royal Society of London A: mathematical, physical and engineering sciences*, vol. 454, no. 1971. The Royal Society, 1998, pp. 903–995.

[17] A. Delorme and S. Makeig, "Eeglab: an open source toolbox for analysis of single-trial eeg dynamics including independent component analysis," *Journal of neuroscience methods*, vol. 134, no. 1, pp. 9–21, 2004.

[18] G. Gómez-Herrero, W. De Clercq, H. Anwar, O. Kara, K. Egiazarian, S. Van Huffel, and W. Van Paesschen, "Automatic removal of ocular artifacts in the eeg without an eog reference channel," in *Proceedings of the IEEE 7th Nordic Signal Processing Symposium,*, 2006, pp. 130–133.

[19] B. Boashash, G. Azemi, and N. A. Khan, "Principles of time-frequency feature extraction for change detection in non-stationary signals: Applications to newborn {EEG} abnormality detection," *Pattern Recognition*, vol. 48, no. 3, pp. 616–627, 2015.

[20] P. Gaur, R. B. Pachori, H. Wang, and G. Prasad, "An empirical mode decomposition based filtering method for classification of motor-imagery eeg signals for enhancing brain-computer interface," in *International Joint Conference on Neural Networks (IJCNN)*, 2015, pp. 1–7.

[21] L. Zhang, C. Zhang, H. Higashi, J. Cao, and T. Tanaka, "Common spatial pattern using multivariate emd for eeg classification," in *Asia-Pacific Signal and Information Processing Association Annual Summit and Conference*, 2011, pp. 244–248.

[22] N. M. El-Kafrawy, D. Hegazy, and M. F. Tolba, "Features extraction and classification of eeg signals using empirical mode decomposition and support vector machine," in *International Conference on Advanced Machine Learning Technologies and Applications*, 2014, pp. 189–198.

[23] P. Flandrin, G. Rilling, and P. Goncalves, "Empirical mode decomposition as a filter bank," *IEEE signal processing letters*, vol. 11, no. 2, pp. 112–114, 2004.

[24] D. Trad, T. Al-Ani, and M. Jemni, "Motor imagery signal classification for bci system using empirical mode décomposition and bandpower feature extraction," *BRAIN. Broad Research in Artificial Intelligence and Neuroscience*, vol. 7, no. 2, pp. 5–16, 2016.

[25] R. Aldea and M. Fira, "Classifications of motor imagery tasks in brain computer interface using linear discriminant analysis," *International Journal of Advanced Research in Artificial Intelligence*, vol. 3, no. 7, pp. 5–9, 2014.

[26] C.-C. Chang and C.-J. Lin, "Libsvm: A library for support vector machines," *ACM Transactions on Intelligent Systems and Technology*, vol. 2, no. 3, pp. 1–27, May 2011.

[27] R. Alazrai, M. Momani, and M. I. Daoud, "Fall detection for elderly from partially observed depth-map video sequences based on view-invariant human activity representation," *Applied Sciences*, vol. 7, no. 4, p. 316, 2017.

[28] R. Alazrai, A. Zmily, and Y. Mowafi, "Fall detection for elderly using anatomical-plane-based representation," in *36th Annual International Conference of the IEEE Engineering in Medicine and Biology Society (EMBC)*, Aug. 2014, pp. 5916–5919.

[29] R. Alazrai, Y. Mowafi, and C. G. Lee, "Anatomical-plane-based representation for human-human interactions analysis," *Pattern Recognition*, vol. 48, no. 8, pp. 2346–2363, 2015.